Journal of Applied Sciences

ISSN 1812-5654

Journal of Applied Sciences 6 (15): 3145-3149, 2006
ISSN 1812-5654

Effect of Aging Temperatures on Impact Toughness of Precipitation Hardening Stainless Steel FV520 (B)

Niu Jing, Dong Junming, Wang Hongyu and Xue Jin
College of Materials Science and Engineering, Xi'an Jiaotong University, No. 28 Xianning Road, Xi'an, 710049, The People's Republic of China

Abstract: TEM microstructure and instrumented impact toughness of precipitation-hardening stainless steel FV520 (B) aged at different temperatures were investigated. The results show that the main precipitate of tested steel is copper-rich phase. After FV520 (B) aged at 420°C, lowest toughness are obtained and the fracture appearance of impact specimens is in the form of cleavage, due to the coherent precipitation of fine copper particles. However, with aging temperature increasing, the strength of steel tested gradually decrease, but its toughness gradually increase and fracture appearance of impact specimens transit to the form of dimple, due to the copper-rich phase precipitating and coarsening, the matrix recrystallizing. Toughness of FV520 (B) at different aging temperatures is dependent on the crack propagation energy. The effect of aging microstructure on impact crack initiation energy is less, but the effect of that on crack propagation energy is great.

Key words: Precipitation-hardening stainless steel, instrumented impact test, aging microstructures

INTRODUCTION

Precipitation-hardened stainless steels were first developed during the 1940 and since then, they have become increasingly important in a variety of applications in which their special properties can be utilized. The most important of these properties are ease of fabrication, high strength, relatively good ductility and excellent corrosion resistance, so the researchers developed new kinds of steels and tried to reveal the hardening mechanism (Guo and Sha, 2003; Habibi Bajguirani, 2002; Nakagawa *et al*., 2000). The FV520 (B) steel is new kind of low-carbon precipitation- hardening stainless steels, which possesses excellent corrosion resistance, better toughness, ideal properties in larger cross-section and good weldability similar to the 18-8 steels, therefore, it has been widely used for gear, bolt, axis, vane, rotor, pump and so on. In China, it has been widely used in blower to produce vanes of high-speed blower used to pump corrosive medium. Relative tests about this kind of steels have also been studied by many researchers. Xiao (1999) pointed out that the heat treatments, especially aging treatment, makes a large effect on the microstructures and tension mechanical properties, but refers few to the toughness. The common impact tests can only get the impact absorbed energy, so that it is hard to reflect the fracture details of the materials under the impact load. However, this problem can be solved by instrumented impact test and the characteristic values of the tests can be given evident physics meanings. With the aging temperature changing, the FV520 (B) steel, as one of the precipitation-hardening stainless steels, undergoes different states of precipitated phase and mocrostructure changing. Therefore, instrumented impact tests make an important sense for revealing toughening mechanism and the detailed toughness change of FV520 (B) aged at different temperature. In this study, the impact cracking process of FV520 (B) aged at different temperature is further investigated by instrumented impact test and fractographic analysis method, in order to provide reference for reasonable utilization and development of precipitation- hardening stainless steels.

MATERIALS AND METHODS

The steel tested was smelted with alkali arc furnace and then performed electroslag refining. The chemical composition of steel tested is shown in Table 1. The steel tested was in the form of plate, 8 mm in thickness.

Table 1: Chemical composition of steel tested (Wt %)

C	Si	Mn	S	P
0.042	0.355	0.579	0.0016	0.017
Ni	Cr	Cu	Mo	Nb
5.540	13.80	1.560	1.470	0.391

Corresponding Author: Niu Jing, College of Materials Science and Engineering, Xi'an Jiaotong University, No. 28 Xianning Road, Xi'an, 710049, The People's Republic of China

FV520 (B) in the as-received condition was solution treated at 1050°C for 2 h followed by air-cooling and aged at 630°C for 3 h followed by air-cooling. In order to get better mechanical properties after aging treatment, intermedial treatment should be first proceeded to evaluate the Ms value and reduce the content of austenite in FV520 (B). As oil quenching at 850°C, the carbides in FV520 (B) in the as-received condition did not solve into austenite, as a result, that heighten Ms of this steel (Xiao, 1999), so oil quenching at 850°C for 2 h was chosen as intermedial treatment process in this study. After intermedial treatment, FV520 (B), respectively aged at 350, 420, 470, 520, 560, 600 and 630°C for 3 h, were investigated.

The impact test were performed on 5×10×55 mm Charpy U-notch impact specimens. The impact test was operated on the TYPE.JBC-300-I instrumented impact testing machine, 300J in standard blow energy, 5.12 m s^{-1} in impact speed, in room temperature. Though various methods about defining the crack initiation loads of the instrumented impact specimens exist, the maximum load recorded during the course of impact test is considered as crack initiation load in this research. The curve of instrumented impact and relative parameters was shown in Fig. 1 (Tosal *et al*., 2000). Here, Fe is elastic load, Fy is yield load, Fm is maximum load, Ai is crack initiation energy, Ap is crack propagation energy, (Ai + Ap) is the total impact energy At.

Fractographic features of impact specimens were examined by means of scanning electron microscopy (SEM) with HITACHI type S-3000N.

The corresponding microstructures were examined by using transmission electron microscopy (TEM). Thin foils for TEM were prepared by mechanical thinning to a thickness of 0.1 mm and followed by electropolishing at 15°C in an electrolyte containing 50 mL of perchloric acid and 450 mL of acetic acid. Those thin foils were examined in a JEM200CX operating at 200 kV.

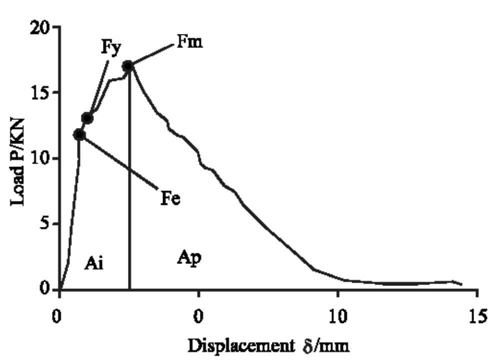

Fig. 1: Curve of instrumented impact test and relative parameters

EXPERIMENTAL RESULTS

Results of instrumented impact test: The instrumented impact test is proceeded using the specimens at the seven aging temperature and three parallel specimens in each plate. During instrumented impact test, the load-displacement curves and relative parameters can be recorded. Six relative parameters are mostly analyzed as follows due to representing characteristic of the load-displacement curves. The curve between six relative parameters and aging temperatures are shown in Fig. 2 and 3. The changing tendency between aging temperature and elastic load Fe, yield load Fy or maximum load Fm are similar. From the Fig. 2, the following rules can be concluded: The three kinds of characteristic loads just reach maximum at 420°C, then fall gradually with the aging temperature ascending and reach the minimum at 600°C and then rise at 630°C. In Fig. 3, crack initiation energy Ai increases slowly with the aging temperature ascending, that shows that the resistance to crack initiation increases with temperature ascending and reaches maximum at 600°C, then falls down at 630°C. However, the crack

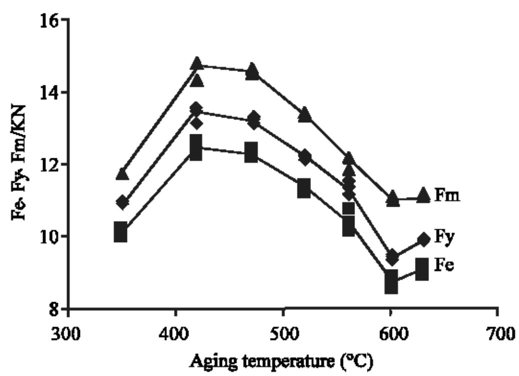

Fig. 2: The effect of aging temperature on the elastic load Fe, yield load Fy and maximum load Fm

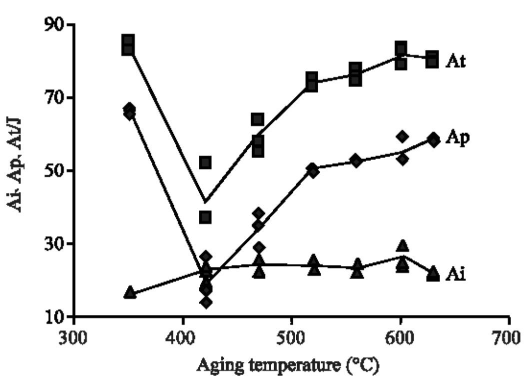

Fig. 3: The effect of aging temperature on crack initiation energy Ai, crack propagation energy Ap and total impact energy At

propagation energy Ap and the total impact energy At appears minimum at aging temperature 420°C and increases in large scale from 420°C to 520°C, then Ap increases slowly with aging temperature from 520°C to 630°C and At reaches the maximum value at 600°C. Moreover, the changing tendencies of the crack propagation energy Ap and the total impact energy At are nearly same and Ap is the main part in total energy At. Figure 3 indicates that the effect of aging temperatures on impact toughness mostly depends on that of aging temperatures on crack propagation energy.

Fractographic analysis: The fracto graph of impact specimens at different aging temperatures are photographed by SEM. The sets of photographs are shown in Fig. 4. SEM feature of impact specimens aged at 420 and 470°C, respectively, are in form of cleavages with large scale of cavities and less shallow dimple existing, as shown in Fig. 4b and c. Hence, it was inferred: at the two aging temperatures, the hardening extent is large, deformation is difficult and the crack propagation are exhibited in an interactive way between cleavage and cavity. The fracture appearance of impact specimens aged at 350, 520, 560, 600 and 630°C, respectively are shown in Fig. 4a-g and the features of the dimples are different, small and shallow dimples containing less precipitated phase in Fig. 4d, large dimples containing large scale of precipitated phase in Fig. 4e and the larger dimples in Fig. 4f representing in better deformation ability. As the results, the toughness of the FV520 (B) steel aged at 600°C is better than that of FV520 (B) aged at 560°C then 520°C. The toughness of the impact specimens aged at 350 and 630°C is better in that the dimples are larger in Fig. 4a, g and the undulation of fracture surface is large.

Observation of aging microstructures: The microstructure of the materials tested oil -quenched at 850°C for 2 h exhibit lath martensite with high-density dislocation. Moreover, less particles within martensite laths was found. TEM-EDX measurements of particles indicates that the particles is niobium-rich carbides. Microstructure of steel tested in the as-received condition is over-aging martensite, so carbides is precipitated within martensite laths. When the steel in the as-received condition was heated only up to 850°C, Nb carbides could not solved into austenite, to retained in martensite laths after oil-quenching.

Figure 5 shows the transmission electron micrographs of the specimens aged at 350, 420, 520, 560, 600 and 630°C for 3 h. In the specimens aged at 350 and 420°C (Fig. 5a and b), other precipitates besides Nb carbides can not be clearly observed due to a high-density dislocation.

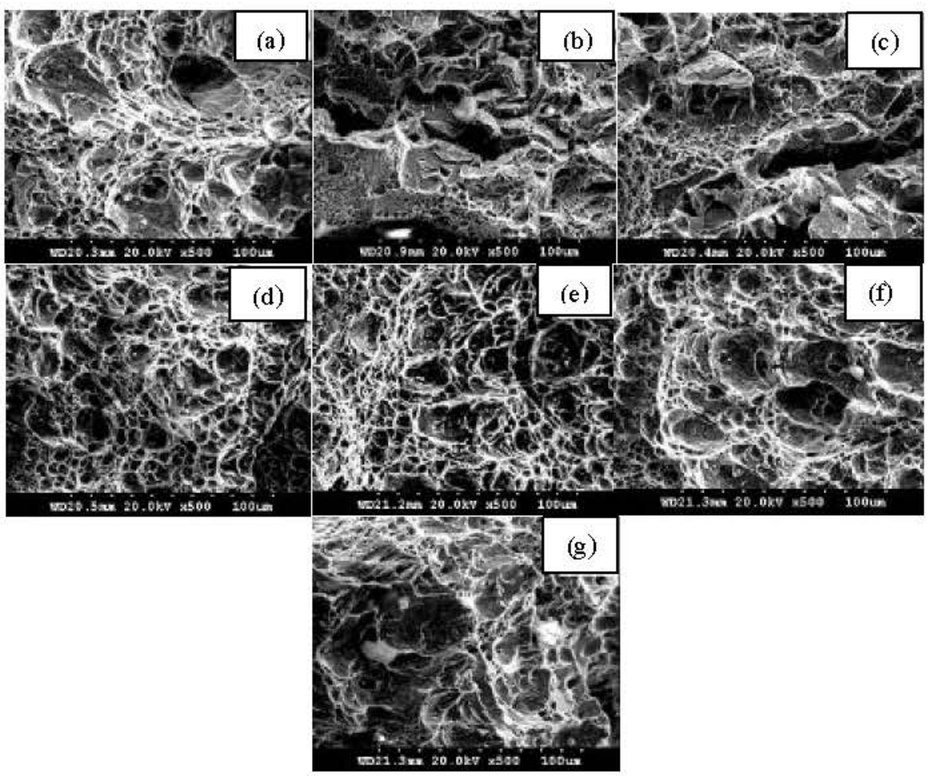

Fig. 4: SEM fractography of impact specimens of FV520 (B) at different aging temperatures (a) 350°C, (b) 420°C, (c) 470°C, (d) 520°C, (e) 560°C, (f) 600°C, (g) 630°C

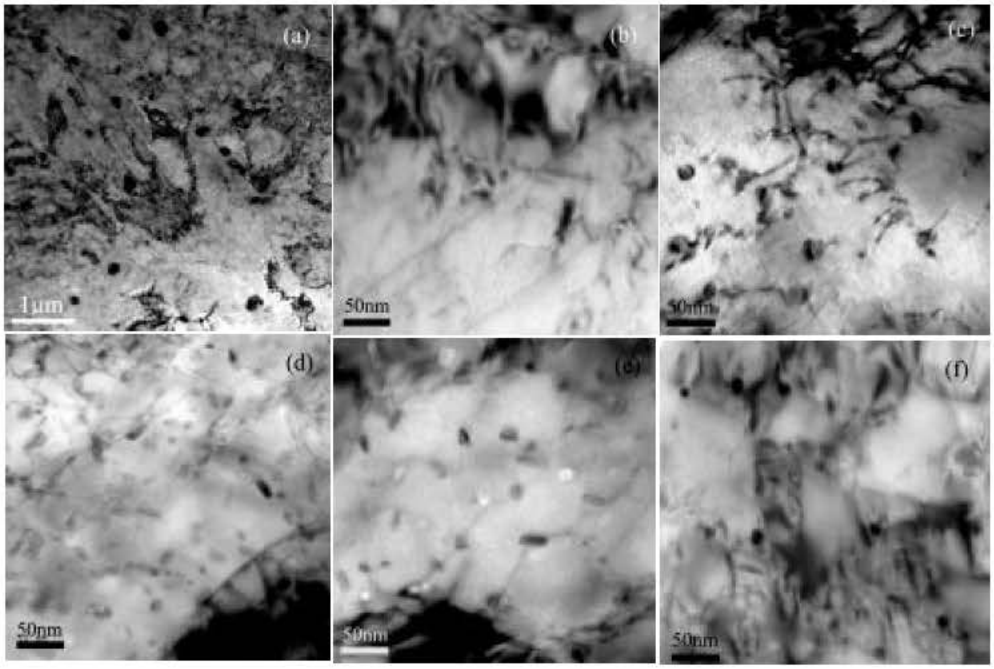

Fig. 5: TEM micrograph of FV520 (B) at different aging temperatures (a) 350°C, (b) 420°C, (c) 520°C, (d) 560°C, (e) 600°C and (f) 630°C

However, smaller coherent precipitates may distribute in the martensite laths, since the increase in Fe, Fy and Fm in Fig. 2 is obtained. The transmission electron micrographs of the martensite lath in the specimens aged at 470°C is not presented in Fig. 1 for being similar with that of 420°C. In the specimens aged at 520°C (Fig. 5c), 560°C (Fig. 5d) and 600°C (Fig. 5e), precipitates can be observed on dislocations. The mean size of precipitates after aging at 600°C even is found to be about 30 nm. Those precipitates were found to be enriched with Cu by means of energy dispersive X-ray spectroscopy equipped in TEM. The precipitates in the specimen aged at 520 and 560°C are considered to be Cu-rich cluster, while the precipitates in the specimens aged at 600°C may be fcc ε-Cu phase on the basis of those sizes. Otherwise, when aging temperature above 520°C, the matrix begain to recrystallize and the content of the retained austenite increases gradually. When aging temperature reaching 600°C, larger precipitated phases produce, the matrix completely recrystallizes and the maximum of retained austenite is reached. The aging temperature reaching 630°C, the secondary quenching martensite laths appear. Above increasing austenite is called inverse austenite.

DISCUSSION

It can be concluded that coherent precipitated phase brings on hardening after 420 and 470°C aged, therefore, in the course of the instrumented impact test, characteristic loads increase and the crack- arrest ability of the dynamic cracks falls down seriously, which makes crack propagation energy descending rapidly and the fracto graph presenting cleavage. Ai Ap and At become more dispersive due to the nonuniform coherent precipitated phases. With the aging temperature ascending, the characteristic loads descend gradually, Ai ascends and Ap increases in a large scale for the reason that the precipitated phase separates and the matrix recrystallizes. Moreover, Nakagawa and Miyazaki (1999) suggest that the increase of the retained austenite makes important role of improving toughness of the precipitation-hardening stainless steels. Therefore, as the aging temperature is above 520°C, the adding of the retained austenite may also improve the toughness. It is inferred that the maximum toughness appears at aging temperature 600°C is because ε-Cu phase enough precipitates, the matrix completely recrystallizes and the maximum retained austenite is reached. Ac1 of the steel is 612°C (Xiao, 1999), so the secondary quenching martensitic microstructure appears when aging at 630°C, to lead to the secondary hardening occurring. Hence, comparing to the aging temperature 600°C, the characteristic load and crack propagation energy Ap increase, but the crack initiation energy Ai decreases. It is inferred that the microstructure containing soft and hard phase makes impact crack initiating easily, but improves the propagated resisting force of the impact cracks.

CONCLUSIONS

- After FV520 (B) aged at 420°C, lowest toughness are obtained, due to the coherent precipitation of fine copper particles. With aging temperatures increasing, the strength of steel tested gradually decrease, but its toughness gradually increase, due to the copper-rich phase precipitating and coarsening, the matrix recrystallizing.
- The effect of aging temperature on the toughness of FV520 (B) steel mainly depends on that of crack propagation energy. With the aging temperature increasing from 420 to 600°C, the crack initiation load decrease gradually, the crack initiation energy increases slowly and the crack propagation energy increases in a large scale.
- The fracture appearances of the impact specimens are cleavages when the specimens aged at 420 and 470°C, or the other are dimples though the dimples is different.

REFERENCES

Guo, Z. and W. Sha, 2003. Vaumousse. Microstructural evolution in a PH13-8 stainless steel after ageing. Acta Materialia, 51: 101-116.

Habibi Bajguirani, H.R., 2002. The effect of ageing upon the microstructure and mechanical properties of type 15-5 PH stainless steel. Materials Sci. Eng., A338: 142-159.

Nakagawa, H. and T. Miyazaki, 1999. Effect of retained austenite on the microstructure and mechanical properties of martensitic precipitation hardening stainless steel. J. Materials Sci., 34: 3901-3908.

Nakagawa, H., T. Miyazaki and H. Yokota, 2000. Effects of aging temperature on the microstructure and mechanical properties of 1.8Cu-7.3Ni-15.9Cr-1.2Mo-lowC,N martensitic precipitation hardening stainless steel. J. Materials Sci., 35: 2245-2253.

Tosal, L., C. Rodriguez and F.J. Belzunce *et al.*, 2000. Comporison of the static and dynamic fracture behaviour of an AE-460 structural steel. Engineering Fracture Mechanics, 66: 537-549.

Xiao, F., 1999. Influence of intermediate treatmenton microstructure and properties of stainless steel Fv520 (B). Transactions of Metal Heat Treatment, 20: 35-40 (In Chinese).